Thermoplastic starch biocomposites reinforced with hemp shives obtained via extrusion

Sylvain Foret, Brahim Mazian, Vassileios Bekas, Felipe C.B. Martins, Osvaldo H Campanella, Patrick Perré, Pedro E.D. Augusto

Foret, S., Mazian, B., Bekas, V., Martins, F. C., Campanella, O. H., Perré, P., & Augusto, P. E. (2023). Thermoplastic starch biocomposites reinforced with hemp shives obtained via extrusion. *Industrial Crops and Products*, *206*, 117707.

https://doi.org/10.1016/j.indcrop.2023.117707

Thermoplastic starch biocomposites reinforced with hemp shives obtained via extrusion

Sylvain Foret[1], Brahim Mazian[1]*, Vassileios Bekas[1,2]; Felipe C. B. Martins[1,3]; Osvaldo H. Campanella[1,4]; Patrick Perré[1,5]; Pedro E. D. Augusto[1]

[1] Université Paris-Saclay, CentraleSupélec, Laboratoire de Génie des Procédés et Matériaux, Centre Européen de Biotechnologie et de Bioéconomie (CEBB), 3 rue des Rouges Terres 51110 Pomacle, France.

[2] Hochschule Bremen, Faculty 5 - School of Nature and Engineering, Neustadtswall 30, 28199 Bremen, Germany.

[3] Institut National des Sciences Appliquées de Rouen (INSA Rouen Normandie), 685 Av. de l'Université, 76800 Saint-Étienne-du-Rouvray, France.

[4] Department of Food Science and Technology, Ohio State University, Columbus, OH, USA.

[5] Université Paris-Saclay, CentraleSupélec, Laboratoire de Génie des Procédés et Matériaux (LGPM), Gif-sur-Yvette, France.

*Corresponding author

Brahim.mazian@centralesupelec.fr

Abstract

Biodegradable and sustainable materials are becoming increasingly important in response to environmental concerns associated with traditional petroleum-based plastics. The objective of this study was to assess the feasibility and efficiency of incorporating hemp shives as a filler in thermoplastic wheat starch, aimed at promoting environmental sustainability and reducing reliance on non-renewable resources. The biocomposites, prepared by extrusion, consisted of pure starch, different hemp shives concentrations (10%, 20%, 30%, 40%, 50%, and 70%), with water and glycerol as plasticizers. The results revealed that the incorporation of shives notably enhanced the mechanical properties of the biocomposite, reaching an optimal performance at 40% shives concentration (resulting in a maximum tensile strength of 11.5 MPa and Young's modulus of 1621 MPa). In this concentration, ESEM images unveiled robust adhesion between hemp shives and the matrix, indicating starch penetration into the shives' parenchymatous cells. At higher concentrations, however, the resulted high pressures during extrusion collapsed the shive cells, impairing their adhesion with starch and reducing the biocomposite strength. The hemp shives addition reduced the water uptake, thereby enhancing the dimensional stability. Conclusively, this study offers pivotal insights into the development and characteristics of starch/hemp shives biocomposites, with structure-process-properties relationships, suggesting their potential applicability in the creation of eco-friendly packaging materials and small objects, presenting a viable alternative to traditional materials.

Keywords: Starch; Hemp shives; bio-based plastic; Morphology; Mechanical properties; Dimensional stability; Water absorption.

1. Introduction

Synthetic plastics from petroleum-based resources are widely used materials in the packaging sector. However, the pervasive use of these materials has raised several environmental concerns, associated with the steady depletion of fossil fuels and the generation of massive non-degradable waste. For this reason, emerging sustainable materials from renewable resources are being developed as an alternative to traditional packaging materials (Asgher et al., 2020; Nie et al., 2018).

Among them, starch is one of the most extensively used renewable biopolymers due to its availability, low price, and biodegradability (Goudarzi et al., 2017; Kremensas et al., 2019; La Fuente et al., 2022). Starch, a complex material with a diverse structure, can be converted into a thermoplastic material through a process that involves the application of heat and mechanical forces in conjunction with water to make the starch granular structure more amorphous and processable, also achievable using a plasticizing agent, like formamide, glucose, sorbitol, or glycerol (Mali, 2008; Maniglia et al., 2021). Using these conditions, starch granules are destructured, plasticized, and melted, forming an amorphous thermoplastic starch (TPS) (Li et al., 2011; La Fuente et al., 2022). However, compared to conventional thermoplastic materials, TPS has some drawbacks that must be overcome, such as its low melting point, low thermal stability, poor mechanical properties, strong capacity to adsorb water and high solubility in water (Donmez et al., 2021; Kim et al., 2015).

Three different approaches can be used to address these constraints. The first approach is to use innovative chemical and physical treatments such as ozone chemical treatment (Castanha et al., 2017), ultrasound (US) technology (Maniglia et al., 2021), dry heating treatment (DHT) (La Fuente et al., 2022; Maniglia et al., 2020) and heat moisture treatment (HMT) (Mathobo et al., 2021). These treatments can alter the physical, morphological, and rheological properties of starch and can introduce new functionalities that are not present in its native starch (Mathobo

et al., 2021). However, the cost of implementing these treatments may be a limiting factor. Additionally, creating materials that are 100% starch-based may have implications for the food industry, as starch is a commonly used food ingredient. Therefore, some authors have proposed a second approach, which involves blending TPS with other biodegradable polymers such as polyvinyl alcohol (PVA), polycaprolactone (PCL), polyhydroxyalkanoates (PHAs), polylactic acid (PLA), polyesteramide (PEA), and aliphatic and aromatic copolyesters. This approach improves the properties of TPS and provides more stable support (Avérous, 2004; Yu et al., 2006). However, it may have limitations due to the dependence of some of the used t polymers on the market petroleum price. Therefore, a third approach, more advantageous, and it would involve adding lignocellulosic biomass particles as a filler to form starch-based biocomposites. This approach is cost-effective, sustainable, and reduces the amount of starch required while improving the final product properties (Ahmad et al., 2020; Avérous, 2004; Chen et al., 2020). It also provides an opportunity for valorizing agricultural wastes.

The chemical structure of starch and lignocellulosic materials enables the formation of hydrogen bonds between these two components (Kumar and Singh, 2008). This results in a strong bond at the matrix-filler interface without the need for additional coupling agents or starch surface modifications. For example, Wollerdorfer and Bader. (1998) increased the tensile strength of TPS from 8.9 MPa to 36.4 MPa when 20% flax fibers were added. By adding 50% of palm mesocarp fiber waste to cassava TPS, Saepoo et al. 2023 obtained biocomposites by compression molding with higher tensile strength, thermal stability, and water resistance. Similar results were obtained by Prachayawarakorn et al. (2010) by adding cotton fibers to thermoplastized rice starch. Cellulose nano or micro-crystals were also proven to be efficient for this purpose, such as improving the starch film performances in terms of mechanical and barrier properties (Othman et al. 2019, Tabassi et al. 2016)

In this study, hemp shives (HS), also called hemp hurds, were used as a filler to wheat TPS polymer, producing a new biocomposite. HS are a byproduct of the hemp fiber production process, which is obtained by removing the outer layer of bast fibers from the stalk of the hemp plant. They are made up of cellulose, hemicelluloses, and lignin, and are considered a waste product from the hemp fiber production process. Hemp fibers are used in various industries, such as pulp and paper and bio-composites for automotive parts (Mazian et al., 2020; Réquilé et al., 2021), whereas HS are mainly used as horse bedding and filler in concrete (hemp concrete, (Jami et al., 2019). Therefore, using HS as a filler, instead of hemp fibers, is an advantageous approach since HS makes up 60-80% of the dry mass of the hemp stem and have no major application, being an inexpensive by-product to be valorized.

This work developed new biocomposites with different hemp shives and wheat TPS concentrations by extrusion. Different properties of the biocomposites were evaluated, to understand the potential applications and describe the interaction between the polymer and particles, including density, morphology, liquid and vapor sorption capacity, hydrophilicity, swelling and mechanical properties.

2. Materials and method

2.1. Raw materials

Biocomposites were prepared using wheat starch, hemp shives (HS), glycerol, and water. Wheat starch (moisture ≤13.0%) was obtained from ADM Starch (Bazancourt, France). Glycerol with 99% purity was purchased from Sigma-Aldrich and used as a plasticizer. HS were provided in bulk by Chanvrière de l'Aube (France). HS particles of 2 to 4 mm were obtained using a Retsch SK 300 miller. Their cellulose (41.9%), hemicelluloses (21.5%), and lignin (26.6%) concentrations were determined using the National Renewable Energy

Laboratory (NREL) standard procedure (Sluiter et al., 2012). The hemp bulk density was around 200 $kg.m^{-3}$.

2.2. Materials processing

Starch powder and liquid were mixed and processed with different proportions of HS using a twin-screw extruder (Haake Polylab Rheomex OS PTW16, D=16mm, L/D=40) coupled with a gravimetric feeder. The liquid was a mixture of glycerol and water at a 62/38 ratio based on the study reported by (La Fuente et al., 2022). Pure wheat starch or starch-HS mixtures with ratios of 0/100%, 10/90%, 20/80%, 30/70%, 40/60%, 50/50% and 70/30% (m/m) were fed into the extruder (Figure 1) at the first module, with an average flow rate of 0.4 kg/h. The liquid mixture was added to the second module via a peristaltic pump, at a rate of 0.1 kg/h. The extrusion formulation was then maintained at a solid-liquid ratio of 80/20 for all experiments. The biocomposite sheets were extruded with a regular temperature profile (60, 75, 90, 100, 110, 110, 110, 110, 105, 100°C, in the 10 zones presented in Figure 1, a slit die (25 mm x 1 mm) and screw speed (100 rpm). Flat material bands (sheets) were produced following each mixing batch process. The screw profile used is schematically shown in Figure 1 and contain several mix zones to achieve a good mixing of the polymers.

2.3. Characterization methods

2.3.1. Density

The density of TPS and biocomposites was determined using the standard mass-over-volume method in accordance with ASTM D792-20. The density was calculated for at least five specimens from each batch to assess reproducibility.

2.3.2. Mechanical properties

Prior to the mechanical tests, both TPS and the biocomposites were conditioned for at least five days at 25°C and 50% relative humidity. Tensile test characterization (ISO 527-3:2018) was then performed on type 1B samples using a computer numerical control (CNC) machine, under the same hygrothermal conditions. Tensile assays were conducted in a universal testing machine (AG-X 100 Shimadzu®) equipped with a non-contact video-type extensometer to determine Young's modulus. The displacement speed was set at 5mm/min until breakage. The tensile strength was calculated as the maximum stress the material can withstand before breaking. To assess reproducibility, tests were performed at least five times for each material.

2.3.3. Morphology analysis

After the mechanical tests, fracture surfaces generated by the tensile were observed by electron microscopy. Images were obtained using an environmental scanning electron microscope (ESEM, Quanta 200, FEI Company) in Low Vac mode, at 133 Pa, voltage 10 kV, with a beam spot size of 4.5 and a working distance of approximately 6 mm. The Low Vac mode allows samples to be imaged without any coating even though they are not electrically conductive. The tension was reduced to limit the beam penetration and the working distance is a compromise between the detector signal and the degradation of the electron beam in a chamber at high pressure. The samples were placed on carbon conductive double-sided adhesive disc, without any further preparation.

2.3.4. Liquid water absorption

Liquid water absorption tests were carried out according to ASTM D570-98. Specimen of dimensions (75mm × 25mm × 1mm) were conditioned for four days at 50°C. The mass measurements were performed after conditioning (t = 0) and after several immersion periods in deionized water (t =1, 2, 3, 4, 5, 24, 48 & 72 hours) at room temperature (24.4 °C + 0.7°C). The

samples length and width were obtained by image evaluation using ImageJ 1.53t (Wayne Rasband (NIH). Therefore, the immersed samples were removed from the water and placed on a transparent flat container (24.4°C, 42%RH). The container was placed on scaled paper and images were taken vertically from 30 cm using a mobile phone camera set on a tripod. Test trials were performed with a caliper to calibrate the ImageJ measurements. The sample thickness was measured using a digital gauge caliper Mitutoyo Digimatic 150 mm (Mitutoyo Europe GmbH, Neuss, Germany). The sample weights were measured after removing unabsorbed water using a dry paper cloth. The mass measurements were performed using a precision balance New Classic MS (Mettler-Toledo, Columbus, Ohio, USA, precision of 0.1 mg). The relative change in weight and volume were measured according to Eq.1 and Eq.2, respectively.

$$M_{Change\%} = \frac{(m_t - m_0)}{m_0} \times 100 \qquad \text{Eq.1}$$

$$V_{Change\%} = \frac{(v_t - v_0)}{v_0} \times 100 \qquad \text{Eq.2}$$

where m_t and v_t are total mass and volume values at time t, m_0 and v_0 are the initial dry sample mass and volume, respectively, obtained at 50°C. The volume was calculated according to Eq.3

$$v_t = length \times width \times thickness \qquad \text{Eq.3}$$

2.3.5. Contact angle with liquid water

The hydrophobicity of TPS and biocomposites was evaluated at ambient temperature using the sessile drop method using the device Digidrop (GBX Scientific LTD, Dublin, Ireland). The experiments were carried out by deposing deionized water on the sample surface using an automatic microsyringe. The drop volume was less than 10 µL to avoid gravitational effects.

Optical CA measurements were performed automatically by the implemented software Visiodrop (Version 1.02.01 GB) on the left and right three-phase-boundary at different time spans (1 s, 100 s, 200 s, and 300 s).

2.3.6. Water vapor sorption

Water vapor sorption tests were conducted using the ProUmid SPSx-1μ system (ProUmid GmbH & Co. KG, Ulm, Germany). This instrument is an advanced, fully automated system designed to measure the water vapor sorption of multiple samples in controlled temperature and relative humidity environments. Sorption isotherms were measured at 25 ± 0.1°C, and relative humidity levels from 0 to 90%, using moisture steps of 30%. The mass and conditions were recorded at intervals of 10 minutes. The equilibrium condition dm/dt was set at 0.0001%/200min. With this demanding value, each RH step took a minimum of 3000 minutes and a maximum of 330 hours for the samples to reach equilibrium. Subsequently, the data were analyzed using the SPS-Toolbox Basic Rel. 1.15 software.

3. Results and discussions

3.1. Density

Figure 2 illustrates changes in the biocomposite density as a function of HS concentration. The addition of HS results in a significant drop in density from 1295 kg/m^3 to 1008 kg/m^3 up to 20% of HS. This is expected as shives are much less dense than starch (ca; 200 kg.m^{-3} against 535 kg.m^{-3}). Then, as the concentration of HS continues to increase, the density of the biocomposite rises to 1151 kg/m^3 for a 70% HS biocomposite. This increase in density is attributed to starch penetration into the shive cells' lumen. As starch fills the void spaces within the shive cells, the overall density of the biocomposite increases due to the higher density of the starch compared to the air initially occupying the voids (confirmed by the ESEM images).

3.2. Mechanical properties

Figure 3 shows a representative tensile test for each value of HS content. The effect of HS content is remarkable, from a ductile behavior for net starch (large deformation and small stress) to more rigid behavior and lower deformation at the break. However, for each test, the initial slope gradually reduces with the strain level until the materials break. The tensile strength (maximum value), Young's modulus (averaged slope in the elastic part), and elongation at break were calculated from the stress-strain curves. The repetitions allowed the distribution of values and a plot box was obtained (Figure 4).

The tensile strength of net TPS was found to be low, approximately 5.5 MPa, with a Young's modulus of 104 MPa and a significant elongation at break of 29.2%. The addition of shives particles gradually increases the tensile strength and the rigidity whereas decreases the elongation at break, specifically up to 40%, for which the best rigidity and tensile stress are obtained with values 1572 MPa and 11 MPa respectively. The elongation at break decreases rapidly up to 20 % HS (29.2 % down to 2.6 %) and then reduces only slightly (2% at 40 % HS).

Above 40% HS, a clear decrease of maximum stress is observed (6.2 MPa at 70%), while the strength is similar at 50 % HS and finally decreases at 70 % (1095 MPa).

As the hemp shives are predominantly composed of lignocellulose, a material that have better mechanical properties in comparison to starch (Ago et al., 2016), the observed increase was expected. However, the results also tell us that beyond a threshold value, the content of starch is no longer sufficient to ensure a good cohesion between the particles and the matrix. Good dispersion and bonding between the HS and the TPS matrix are essential to enhance the mechanical properties of the samples. Other researchers reported similar results when adding other lignocellulosic materials, such as rose residue, jute strands, and kenaf fibers, in starch matrices (Ibrahim et al., 2020; Vilaseca et al., 2007; Wollerdorfer and Bader, 1998; Zainuddin et al., 2013). Therefore, these findings suggest that the use of lignocellulosic materials as

reinforcement agents can offer a promising approach to enhancing the performance of starch-based biocomposites. Microscopic observations of the ruptured surfaces provide a more detailed visual information on the effects of HS in the biocomposites.

3.3. Fracture surface morphology

Figure 5 displays the fracture surface morphology of TPS and HS-reinforced TPS biocomposites for different HS contents (10 %, 30 %, 50 % and 70 %). Figure 5a shows that TPS sample has a smooth and undulating surface. Figure 5c shows the biocomposite with 10% HS. At this HS/TPS ratio, the HS particles are dispersed into the polymeric matrix of wheat starch which is a very connected phase. The fracture surface shows a large particle aligned along the surface and two cavities produced by the detachment of two particles, that remained in the other part of the sample (see red arrows). The interface between the particles and the matrix is clearly the weak part of the composite.

Figures 5c-e show the biocomposite with 30% HS. Figures 5c and 5d reveal a uniform distribution of shives throughout the matrix, and a heterogeneous but quite flat fracture surface. Unlike the 10% HS biocomposite fractures arise either inside a particle (the flat surface demostrates that the fracture surface passes through the particle instead the interface, see Figure 5c). This observation remains valid even when the particle is aligned along the tensile direction (Figure 5e). This is more surprising as the strength of shives is much higher in its longitudinal direction. All these observations prove that the interface between the particles and the matrix is very strong and never is the weak point of the composite. This is explained by the penetration of starch inside the cellular lumens in the peripheral zones of shive particles. The microscopy observations provide a clear explanation why a defined content of shives improves the mechanical behavior of the biocomposites.

At 50% of HS, the fracture surface becomes rough and shows a uniform distribution of particles. Zones with only matrix disappeared (Figure 5f), which confirms that the amount of

starch can no longer nicely envelop all the particles. At this level of starch/HS ratio, the HS particles seem also to be shredded during extrusion, a possible consequence of a higher global viscosity due to the reduced lubrication role of starch. For instance, the arrows in Figure 5f indicate a shive particle that have been twisted during extrusion.

These trends are even more obvious in 70 % of HS. The lack of matrix to cover all surfaces of the HS is evidenced in Figure 5g. The further increase of viscosity now completely collapses the cellular structure of shives to such a level that the cell lumens disappeared (Figure 5h). In spite of the increased density, this collapse weakens the particles themselves as can be seen in the figure (see arrows). Both the poor interface and the weak particle explain the weak tensile strength observed in the mechanical tests.

3.4. Contact angle for liquid water

Figure 6 illustrates the contact angles measured on the neat TPS and the biocomposites containing different HS contents at different times (1 s, 100 s, 200 s and 300 s). Careful observation of the images indicates that the triple point remains at the same position over time, confirming that there is no additional wetting of the drop. Then, the value obtained at short time (1 s, in this case) represents the actual contact angle, while the evolution over time is related to the ability of water to penetrate the material.

Globally, the contact angles of the TPS and biocomposite samples were less than 90°, which means that water is the wetting fluid and that the surfaces are hydrophilic. By increasing the content ion of HS in the TPS matrix, the contact angle increases from 55° until its peak (65°) obtained at 40% HS. After 40 %, the contact angle decreases again.

The variations in the measure angle remain low and could be explained by the presence of two hydrophilic phases (hemp and starch). The slight decrease in wettability at intermediate HS contents could be simply explained by the roughness of the surface. At very high HS

contents, the high affinity of hemp shives to water probably compensates for the surface roughness.

The time evolution of the angle shows quasi-parallel curves. The ability of water to penetrate in the material does not seem to be affected by the content of HS. Identical behavior has been reported by (Chen et al., 2020), who observed observing an increase in contact angle from 57° to 72° by adding microcrystalline cellulose to TPS. Similarly, Cao et al., 2008 observed an increase from 39.5° to 66.5° after adding 30% of hemp nanocrystals to plasticized starch. However, these two papers reported results obtained with hydrophobic micro-particles, which is not directly comparable with our results.

3.5. Liquid water absorption and swelling

One of the significant drawbacks of starch-based materials is their propensity to water absorption (liquid and vapor). Figure 7 shows the results of liquid water uptake as a function of storage time. All curves exhibit a rapid initial uptake (ca. 5 hours) rate followed by a plateau. Consistently, the swelling curves exhibited a similar shape. The presence of shives dramatically reduces both the quantity of absorbed water and the swelling at the plateau, while the first transient period seems to have the same dynamics. One could hypothesize that this is due to a lower propensity of shive to attract water, but this is not enough to explain the behavior as the observations are not additive. For example, the water uptake reaches 300 % for the net TPS and drops to 100 % for samples containing 50% shives. The high lignin content and wax of hemp shives (Hill et al., 2009) could explain the small water uptake of HS. However, even assuming shives to take not water at all, which is unrealistic, the water uptakes should have been close to 150 %. However, our interpretation is different and is due to the presence of shives that promote the formation of rigid part regions in the composite with very low swelling (indeed quasi-absence of swelling in their length) and constrains the "free" swelling of starch. This in turn, limits its amount of absorbed water. It is worth mentioning that contrary to all previous

properties measured so far in this work, the effect of HS content remains monotonic up to the maximum content of 70 %.

These results are in line with those obtained in the literature. For instance, Svagan et al. (2009) found that incorporating wood nanofiber into potato starch films decreased its moisture diffusivity and maximum moisture absorption. This was also observed with the inclusion of macroscopic particles, like in our work, for example by adding jute and kapok fibers to thermoplastic cassava starch composites (Prachayawarakorn et al., 2013). Similarly, Lomelí Ramírez et al. 2011 reported a linear decrease in swelling of the composite with increasing of green coir fiber reinforcement to cassava starch.

3.6. Moisture sorption

Moisture sorption is a critical factor that can impact the performance of biocomposites, as it reflects their interaction with water vapor present in the atmosphere. The results indicate that both the net TPS matrix and TPS biocomposites containing different amounts of HS have the ability to absorb significant amounts of moisture when exposed to 90% relative humidity (Figure 8). Pure starch has a sorption capacity of 50%, while the biocomposites exhibit slightly lower sorption capacities, ranging from 42-45% moisture content at 90 % RH, depending on the concentrations of HS. These findings suggest that the addition of HS to the starch matrix has a minor effect on the moisture sorption capacity of the biocomposites. Moura et al. 2021 observed that the addition of babassu coconut fibers resulted in a slight decrease in moisture sorption. At 50% humidity, the moisture content was 29.7% for TPS, 28.6% for biocomposites containing treated fibers, and 27.9% for biocomposites containing untreated fibers. Similarly, Corradini et al. 2008 found that the addition of 5% to 30% sisal fibers to TPS resulted in a stable moisture content of 9-10% when stored at 52% relative humidity. However, when the relative humidity increased to 97%, the moisture content decreased from 35% for TPS to 29% for the biocomposite containing30% sisal.

3.7. Final considerations: integrating mechanisms

The full set of data collected on the hemp-starch composites with various hemps-shives contents allows to define detailed mechanisms describing the evolution of the physicochemical properties of the composites (Figure 9 and Table 1S). These composites consist of hemp particles bound by a starch matrix. Starch is a material with a medium density (535kg/m^3), low mechanical properties, high affinity by water and a huge swelling. By contrast, hemp shives have a low density, good mechanical properties, and excellent dimensional stability in high relative humidity environments. However, the properties of the composite depend on the matrix/particle interface and on possible alterations of these materials during manufacturing.

The addition of particles changes the rheology of the mixture, and the pressure increases with HS content, except at a content of 10% for which a reduced pressure was obtained (one can imagine that a few particles might reduce friction at the solid parts). The ESEM images revealed that this pressure is of key importance and at a certain threshold value, penetration of starch inside the particles is promoted, which reinforced the matrix/particle interface. However, at a higher pressure, the collapse of the shives cellular structure is triggered, which, ultimately, is total at 70 % HS. The variation of density is perfectly consistent. At low HS contents, the composite density is reduced due to the small density of shives, without penetration into the strach matrix and without collapse. As the pressure increases, penetration in shive pores, together with cell collapse explains the increase in density. The observed mechanical properties are also a consequence of this. At low contents (10% and 20%), the interface between these components is the weak point of the composite. Further increasing the HS content, the pressure increases and forced starch to penetrate inside the cell lumens of shives, which reinforce the interface. Above an optimal value, the pressure further increases, completely collapses and

weakens the cellular structure of shives, while starch is not enough to ensure good bonding. The best properties are obtained for a HS content of 40 % to 50 % (depending on whether stiffness or strength is the most important mechanical parameter being considered). The effect of HS content on the wetting contact angle and sorption isotherm is moderate to negligible and therefore is not a criterion to choose the best strach/HS ratios. On the contrary, the effect of HS content on swelling after immersion in water is very beneficial and monotonic (the benefit continues up to 70 % HS). In conclusion, the recommended content of hemp shives is in the range of 40 % to 50 % for the best compromise between mechanical properties and dimensional stability. If the objective is to save starch for applications that require limited water uptake and swelling, we recommend using composite with higher HS contents (70 %).

The understanding of the global behavior of composites containing hemp-shives during manufacturing and during use, will be applied to different composites or to further improved the product.

4. Conclusions

Biocomposites based on hemp shives incorporated in wheat thermoplastic starch were produced by extrusion and their physicochemical and mechanical properties were characterized to obtain bio-based materials with good performances as a way to valorize agro-industrial by-products.

The effect of increasing shives content (10%, 20%, 30%, 40%, 50% and 70%) were evaluated on the density, mechanical properties, morphology, and interaction of biocomposites with liquid and vapor water. Structure-process-properties relationships were developed to explain the observed behavior. These in-depth analyses and comprehensive data sets elucidate the evolution of properties, showcasing the reinforcing capacity of moderate hemp shives content through starch penetration at the interface, the structural collapse due to high processing pressure at higher shives contents, and the advantageous dimensional stability and water uptake

of the samples. The results highlight that the optimal balance between mechanical properties and dimensional stability is achieved with 40 to 50% of hemp shives content, presenting an effective compromise. Higher contents, while advantageous for starch economization and dimensional stability, exhibit a reduction in mechanical strength.

In conclusion, the produced biocomposites have the potential to be a potential alternative to address the growing environmental concerns associated with traditional petroleum-based plastics. Using hemp shives as a filler can also reduce the cost of the final product. Overall, the produced biocomposite represents a promising step towards the production of more sustainable, environmentally friendly, and cost-effective materials.

Author contributions

Sylvain Foret: Conceptualization; Methodology; Validation; Formal analysis; Investigation; Data Curation Management; Writing – Original Draft; Visualization.
Brahim Mazian: Conceptualization; Methodology; Validation; Formal analysis; Investigation; Data Curation Management; Writing – Original Draft; Visualization.
Vassileios Bekas: Validation; Formal analysis; Investigation; Data Curation Management.
Felipe C. B. Martins: Validation; Formal analysis; Investigation; Data Curation Management.
Osvaldo H. Campanella: Methodology; Writing - Review & Editing.
Patrick Perré: Conceptualization; Methodology; Formal analysis; Investigation; Resources; Data Curation Management; Writing - Review & Editing; Supervision; Project administration; Funding acquisition.
Pedro E. D. Augusto: Conceptualization; Methodology; Formal analysis; Writing - Review & Editing; Supervision; Project administration.

Acknowledgments

Communauté urbaine du Grand Reims, Département de la Marne, Région Grand Est and European Union (FEDER Champagne-Ardenne 2014-2020) are acknowledged for their financial support to the Chair of Biotechnology of CentraleSupélec and the Centre Européen de

Biotechnologie et de Bioéconomie (CEBB). Prof. Osvaldo H. Campanella was Visiting Professor through a program of the Direction de la Recherche de CentraleSupélec.

References

Ago, M., Ferrer, A., Rojas, O.J., 2016. Starch-Based Biofoams Reinforced with Lignocellulose Nanofibrils from Residual Palm Empty Fruit Bunches: Water Sorption and Mechanical Strength. ACS Sustainable Chem. Eng. 4, 5546–5552. https://doi.org/10.1021/acssuschemeng.6b01279

Ahmad, A.N., Lim, S.A., Navaranjan, N., Hsu, Y.-I., Uyama, H., 2020. Green sago starch nanoparticles as reinforcing material for green composites. Polymer 202, 122646. https://doi.org/10.1016/j.polymer.2020.122646

Asgher, M., Qamar, S.A., Bilal, M., Iqbal, H.M.N., 2020. Bio-based active food packaging materials: Sustainable alternative to conventional petrochemical-based packaging materials. Food Research International 137, 109625. https://doi.org/10.1016/j.foodres.2020.109625

ASTM D570-98. Test Method for Water Absorption of Plastics. ASTM International. https://doi.org/10.1520/D0570-98R18

ASTM D792-20. Test Methods for Density and Specific Gravity (Relative Density) of Plastics by Displacement. ASTM International. https://doi.org/10.1520/D0792-20

Avérous, L., 2004. Biodegradable Multiphase Systems Based on Plasticized Starch: A Review. Journal of Macromolecular Science, Part C: Polymer Reviews 44, 231–274. https://doi.org/10.1081/MC-200029326

Cao, X., Chen, Y., Chang, P.R., Stumborg, M., Huneault, M.A., 2008. Green composites reinforced with hemp nanocrystals in plasticized starch. J. Appl. Polym. Sci. 109, 3804–3810. https://doi.org/10.1002/app.28418

Castanha, N., Matta Junior, M.D. da, Augusto, P.E.D., 2017. Potato starch modification using the ozone technology. Food Hydrocolloids 66, 343–356. https://doi.org/10.1016/j.foodhyd.2016.12.001

Chen, J., Wang, X., Long, Z., Wang, S., Zhang, J., Wang, L., 2020. Preparation and performance of thermoplastic starch and microcrystalline cellulose for packaging composites: Extrusion and hot pressing. International Journal of Biological Macromolecules 165, 2295–2302. https://doi.org/10.1016/j.ijbiomac.2020.10.117

Corradini, E., Agnelli, J.A.M., Morais, L.C. de, Mattoso, L.H.C., 2008. Estudo das propriedades de compósitos biodegradáveis de amido/glúten de milho/glicerol reforçados com fibras de sisal. Polímeros 18, 353–358. https://doi.org/10.1590/S0104-14282008000400016

Donmez, D., Pinho, L., Patel, B., Desam, P., Campanella, O.H., 2021. Characterization of starch–water interactions and their effects on two key functional properties: starch gelatinization and retrogradation. Current Opinion in Food Science 39, 103–109. https://doi.org/10.1016/j.cofs.2020.12.018

Goudarzi, V., Shahabi-Ghahfarrokhi, I., Babaei-Ghazvini, A., 2017. Preparation of ecofriendly UV-protective food packaging material by starch/TiO2 bio-nanocomposite: Characterization. International Journal of Biological Macromolecules 95, 306–313. https://doi.org/10.1016/j.ijbiomac.2016.11.065

Hill, C.A.S., Norton, A., Newman, G., 2009. The water vapor sorption behavior of natural fibers. J. Appl. Polym. Sci. 112, 1524–1537. https://doi.org/10.1002/app.29725

Ibrahim, M.M., Moustafa, H., Rahman, E.N.A.E., Mehanny, S., Hemida, M.H., El-Kashif, E., 2020. Reinforcement of Starch Based Biodegradable Composite Using Nile Rose Residues. Journal of Materials Research and Technology 9, 6160–6171. https://doi.org/10.1016/j.jmrt.2020.04.018

ISO 527-3:2018, 2018. Plastiques — Détermination des propriétés en traction — Partie 3: Conditions d'essai pour films et feuilles. ISO.

Jami, T., Karade, S.R., Singh, L.P., 2019. A review of the properties of hemp concrete for green building applications. Journal of Cleaner Production 239, 117852. https://doi.org/10.1016/j.jclepro.2019.117852

Kim, S.R.B., Choi, Y.-G., Kim, J.-Y., Lim, S.-T., 2015. Improvement of water solubility and humidity stability of tapioca starch film by incorporating various gums. LWT - Food Science and Technology 64, 475–482. https://doi.org/10.1016/j.lwt.2015.05.009

Kremensas, A., Kairytė, A., Vaitkus, S., Vėjelis, S., Balčiūnas, G., 2019. Mechanical Performance of Biodegradable Thermoplastic Polymer-Based Biocomposite Boards from Hemp Shivs and Corn Starch for the Building Industry. Materials 12, 845. https://doi.org/10.3390/ma12060845

Kumar, A.P., Singh, R.P., 2008. Biocomposites of cellulose reinforced starch: Improvement of properties by photo-induced crosslinking. Bioresource Technology 99, 8803–8809. https://doi.org/10.1016/j.biortech.2008.04.045

La Fuente, C.I.A., do Val Siqueira, L., Augusto, P.E.D., Tadini, C.C., 2022. Casting and extrusion processes to produce bio-based plastics using cassava starch modified by the dry heat treatment (DHT). Innovative Food Science & Emerging Technologies 75, 102906. https://doi.org/10.1016/j.ifset.2021.102906

Li, M., Liu, P., Zou, W., Yu, L., Xie, F., Pu, H., Liu, H., Chen, L., 2011. Extrusion processing and characterization of edible starch films with different amylose contents. Journal of Food Engineering 106, 95–101. https://doi.org/10.1016/j.jfoodeng.2011.04.021

Lomelí Ramírez, M.G., Satyanarayana, K.G., Iwakiri, S., de Muniz, G.B., Tanobe, V., Flores-Sahagun, T.S., 2011. Study of the properties of biocomposites. Part I. Cassava starch-green coir fibers from Brazil. Carbohydrate Polymers 86, 1712–1722. https://doi.org/10.1016/j.carbpol.2011.07.002

Mali, S., 2008. Antiplasticizing effect of glycerol and sorbitol on the properties of cassava starch Films. Braz. J. Food Technol. 11.

Maniglia, B.C., Castanha, N., Le-Bail, P., Le-Bail, A., Augusto, P.E.D., 2021. Starch modification through environmentally friendly alternatives: a review. Critical Reviews in Food Science and Nutrition 61, 2482–2505. https://doi.org/10.1080/10408398.2020.1778633

Maniglia, B.C., Lima, D.C., da Matta Júnior, M., Oge, A., Le-Bail, P., Augusto, P.E.D., Le-Bail, A., 2020. Dry heating treatment: A potential tool to improve the wheat starch properties for 3D food printing application. Food Research International 137, 109731. https://doi.org/10.1016/j.foodres.2020.109731

Mathobo, V.M., Silungwe, H., Ramashia, S.E., Anyasi, T.A., 2021. Effects of heat-moisture treatment on the thermal, functional properties and composition of cereal, legume and tuber starches—a review. J Food Sci Technol 58, 412–426. https://doi.org/10.1007/s13197-020-04520-4

Mazian, B., Bergeret, A., Benezet, J.-C., Malhautier, L., 2020. Impact of field retting and accelerated retting performed in a lab-scale pilot unit on the properties of hemp fibres/polypropylene biocomposites. Industrial Crops and Products 143, 111912. https://doi.org/10.1016/j.indcrop.2019.111912

Moura, C.V.R. de, Sousa, D. da C., Moura, E.M. de, Araújo, E.C.E. de, Sittolin, I.M., 2021. New biodegradable composites from starch and fibers of the babassu coconut. Polímeros 31, e2021007. https://doi.org/10.1590/0104-1428.09519

Nie, S., Zhang, K., Lin, X., Zhang, C., Yan, D., Liang, H., Wang, S., 2018. Enzymatic pretreatment for the improvement of dispersion and film properties of cellulose nanofibrils. Carbohydrate Polymers 181, 1136–1142. https://doi.org/10.1016/j.carbpol.2017.11.020

Othman, S.H., Majid, N.A., Tawakkal, I.S.M.A., Basha, R.K., Nordin, N., Shapi'I, R.A., 2019. Tapioca starch films reinforced with microcrystalline cellulose for potential food packaging application. Food Sci. Technol 39, 605–612. https://doi.org/10.1590/fst.36017

Prachayawarakorn, J., Chaiwatyothin, S., Mueangta, S., Hanchana, A., 2013. Effect of jute and kapok fibers on properties of thermoplastic cassava starch composites. Materials & Design 47, 309–315. https://doi.org/10.1016/j.matdes.2012.12.012

Prachayawarakorn, J., Sangnitidej, P., Boonpasith, P., 2010. Properties of thermoplastic rice starch composites reinforced by cotton fiber or low-density polyethylene. Carbohydrate Polymers 81, 425–433. https://doi.org/10.1016/j.carbpol.2010.02.041

Réquilé, S., Mazian, B., Grégoire, M., Musio, S., Gautreau, M., Nuez, L., Day, A., Thiébeau, P., Philippe, F., Chabbert, B., Chamussy, A., Shah, D.U., Beaugrand, J., Placet, V., Benezet, J.-C., le Duigou, A., Bar, M., Malhautier, L., De Luycker, E., Amaducci, S., Baley, C., Bergeret, A., Bourmaud, A., Ouagne, P., 2021. Exploring the dew retting feasibility of hemp in very contrasting European environments: Influence on the tensile mechanical properties of fibres

and composites. Industrial Crops and Products 164, 113337. https://doi.org/10.1016/j.indcrop.2021.113337

Saepoo, T., Sarak, S., Mayakun, J., Eksomtramage, T., Kaewtatip, K., 2023. Thermoplastic starch composite with oil palm mesocarp fiber waste and its application as biodegradable seeding pot. Carbohydrate Polymers 299, 120221. https://doi.org/10.1016/j.carbpol.2022.120221

Sluiter, A., Sluiter, J., Templeton, D., Crocker, D., Ruiz, R., Hames, B., Scarlata, C., 2012. Determination of structural carbohydrates and lignin in biomass. National Renewable Energy Laboratory-NREL. TP-510-42618 Laboratory Analytical Procedure (LAP) Golden, CO.

Svagan, A.J., Hedenqvist, M.S., Berglund, L., 2009. Reduced water vapour sorption in cellulose nanocomposites with starch matrix. Composites Science and Technology 69, 500–506. https://doi.org/10.1016/j.compscitech.2008.11.016

Tabassi, N., Moghbeli, M.R., Ghasemi, I., 2016. Thermoplastic starch/cellulose nanocrystal green composites prepared in an internal mixer. Iran Polym J 25, 45–57. https://doi.org/10.1007/s13726-015-0398-0

Vilaseca, F., Mendez, J.A., Pèlach, A., Llop, M., Cañigueral, N., Gironès, J., Turon, X., Mutjé, P., 2007. Composite materials derived from biodegradable starch polymer and jute strands. Process Biochemistry 42, 329–334. https://doi.org/10.1016/j.procbio.2006.09.004

Wollerdorfer, M., Bader, H., 1998. Influence of natural fibres on the mechanical properties of biodegradable polymers. Industrial Crops and Products 8, 105–112. https://doi.org/10.1016/S0926-6690(97)10015-2

Yu, L., Dean, K., Li, L., 2006. Polymer blends and composites from renewable resources. Progress in Polymer Science 31, 576–602. https://doi.org/10.1016/j.progpolymsci.2006.03.002

Zainuddin, S.Y.Z., Ahmad, I., Kargarzadeh, H., Abdullah, I., Dufresne, A., 2013. Potential of using multiscale kenaf fibers as reinforcing filler in cassava starch-kenaf biocomposites. Carbohydrate Polymers 92, 2299–2305. https://doi.org/10.1016/j.carbpol.2012.11.106

Highlights

- ✓ Hemp shives and wheat thermoplastic starch biocomposites showed good performances.
- ✓ Hemp shives improve mechanical properties up to a certain concentration.
- ✓ ESEM images revealed the role of starch penetration to particle/matrix adhesion.
- ✓ Optimal range of shives content is 40-50%, balancing strength and dimensional stability.
- ✓ The optimal range is explained by the effect of shives content on starch penetration.

Figures :

Figure 1

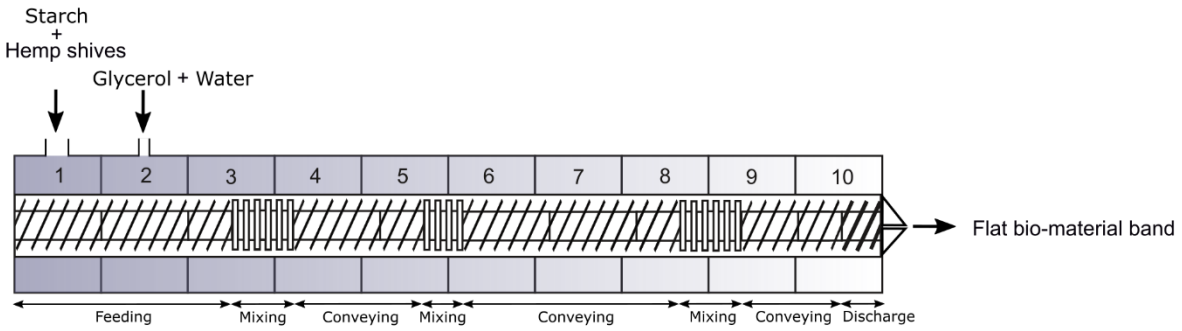

Figure 1. Schematic illustration of the extruder barrel, with its 10 zones of temperature control, and screw profile.

Figure 2

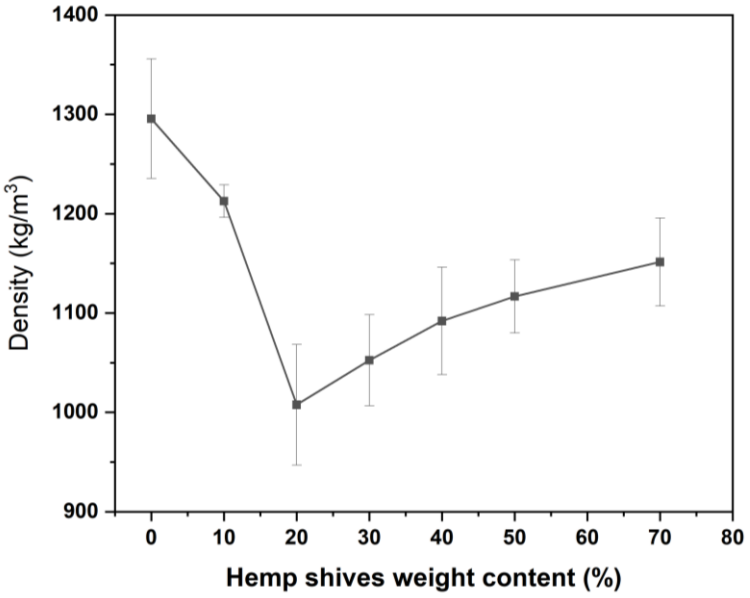

Figure 2. Densities of biocomposites for different hemp shive / wheat starch ration. Symbols are averages and bars are the associated standard deviations.

Figure 3

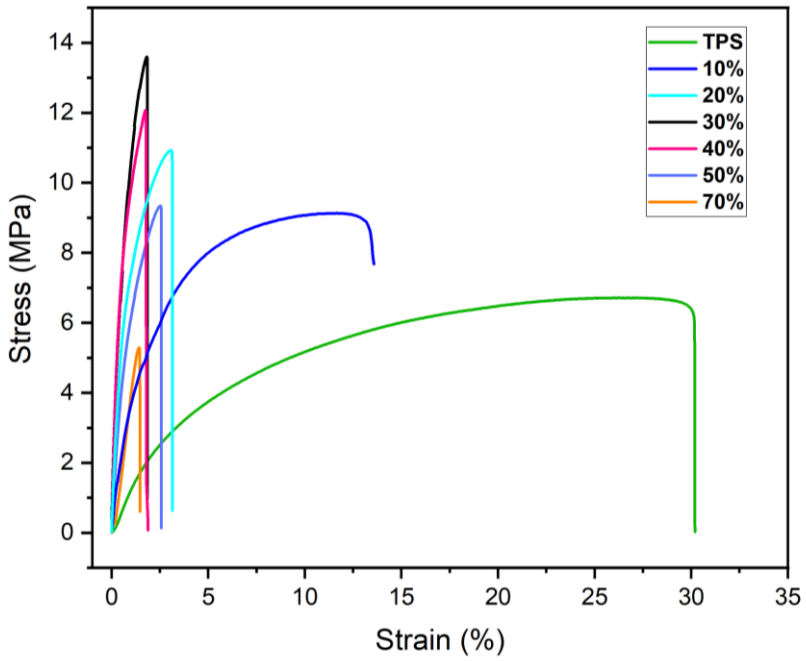

Figure 3: Stress as a function of strain for TPS and different biocomposites (10%, 20%, 30%, 40%, 50% and 70%)

Figure 4

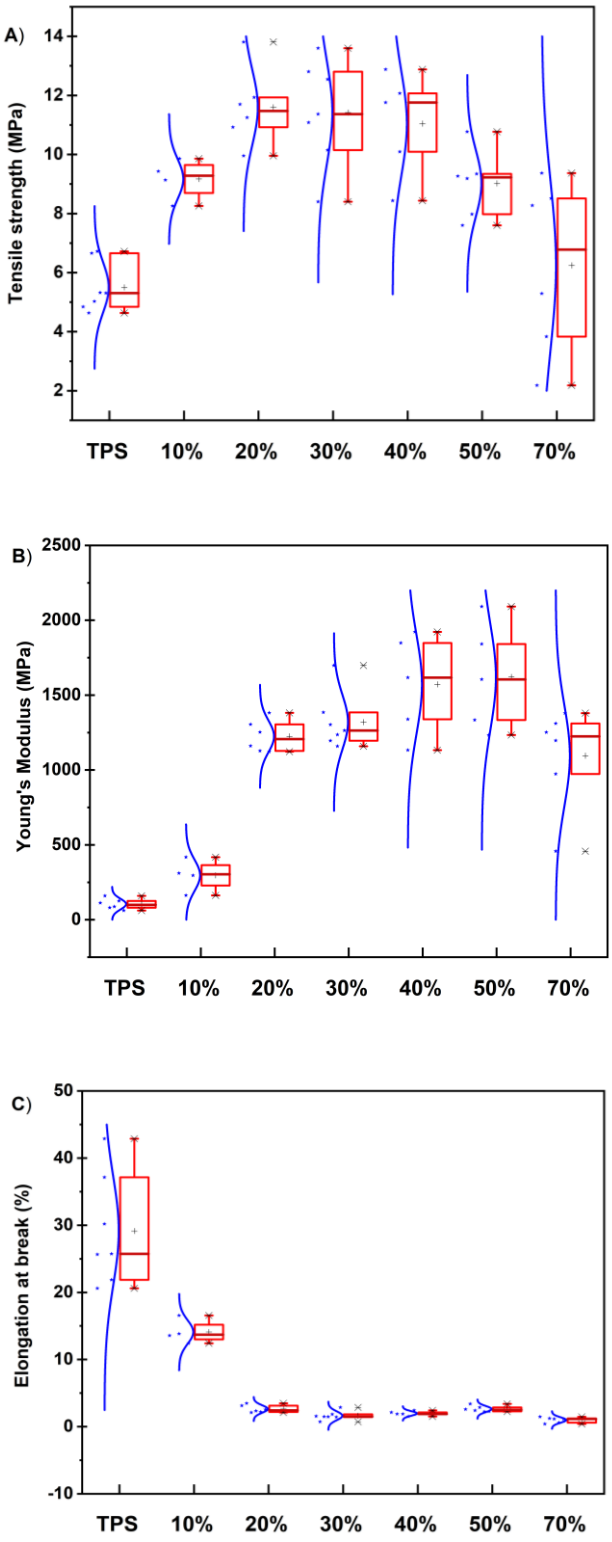

Figure 4: Results of tensile strength (A), Young's modulus (B), and elongation at break (C) for neat TPS and biocomposites with different HS loading.

Figure 5

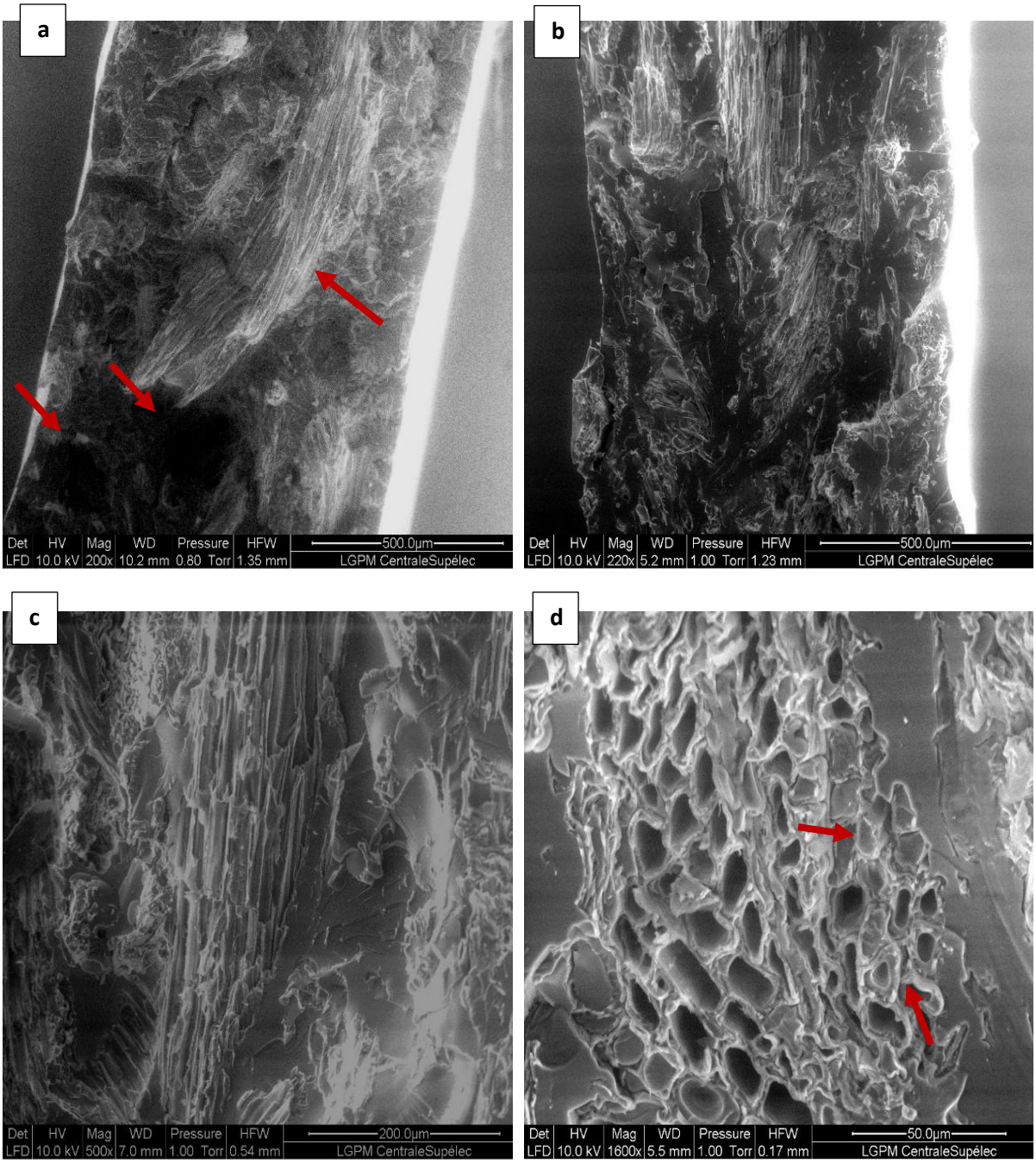
a
Det HV Mag WD Pressure HFW
LFD 10.0 kV 200x 10.2 mm 0.80 Torr 1.35 mm
500.0µm
LGPM CentraleSupélec
b
Det HV Mag WD Pressure HFW
LFD 10.0 kV 220x 5.2 mm 1.00 Torr 1.23 mm
500.0µm
LGPM CentraleSupélec
c
Det HV Mag WD Pressure HFW
LFD 10.0 kV 500x 7.0 mm 1.00 Torr 0.54 mm
200.0µm
LGPM CentraleSupélec
d
Det HV Mag WD Pressure HFW
LFD 10.0 kV 1600x 5.5 mm 1.00 Torr 0.17 mm
50.0µm
LGPM CentraleSupélec

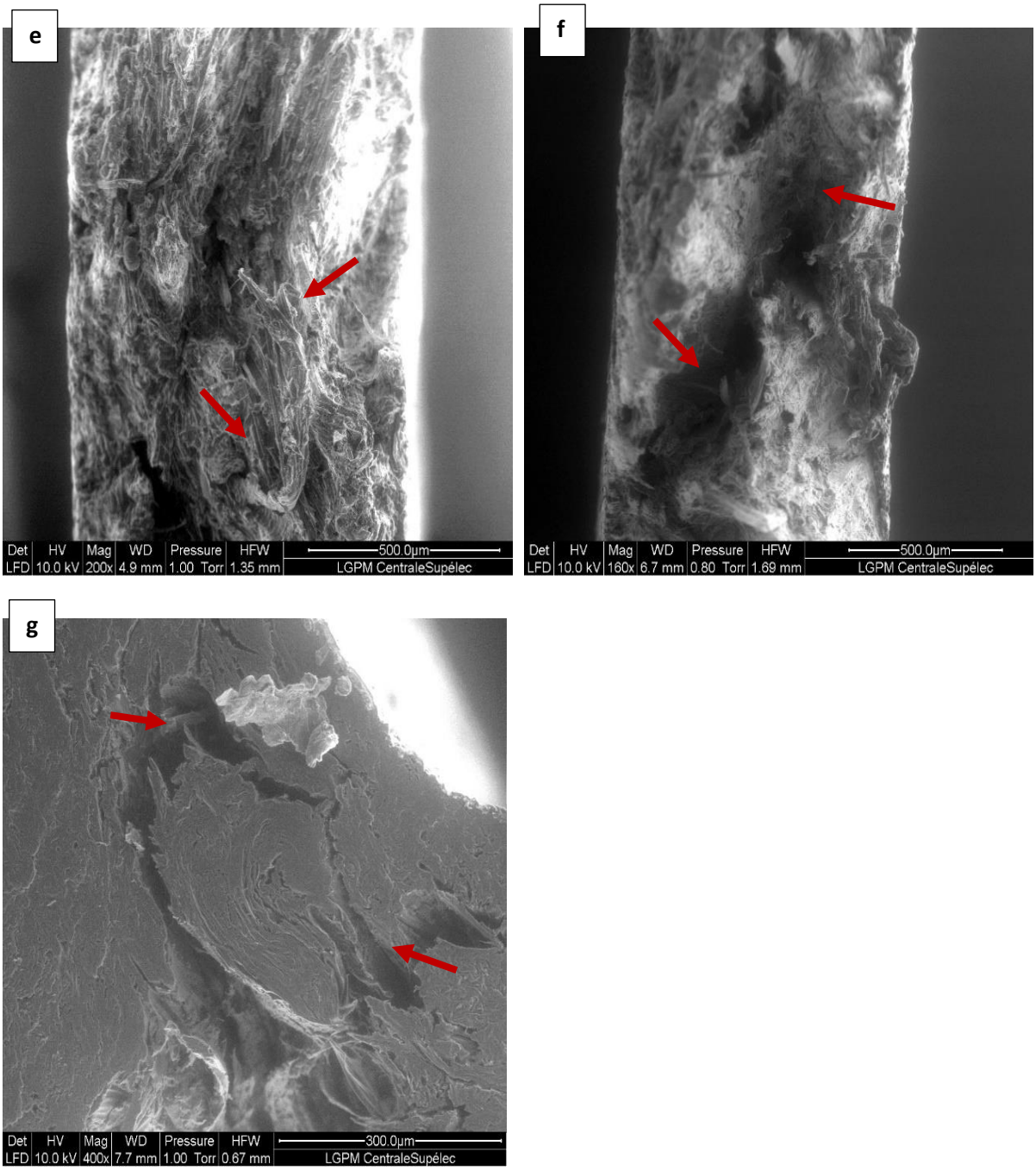

Figure 5: ESEM micrographs of the fractured surface of the thermoplastic starch matrix and filled with different hemp shives ratios: (a) 10% HS; (b) 30% HS. (c) detail of HS-matrix interface for 30% HS; (d) hemp fracture and its cellular structure for 30% HS; (e) 50% HS; (f) 70% HS; g) detail of hemp–matrix interface for 70% HS. The arrows indicate points of discussion in the text.

Figure 6

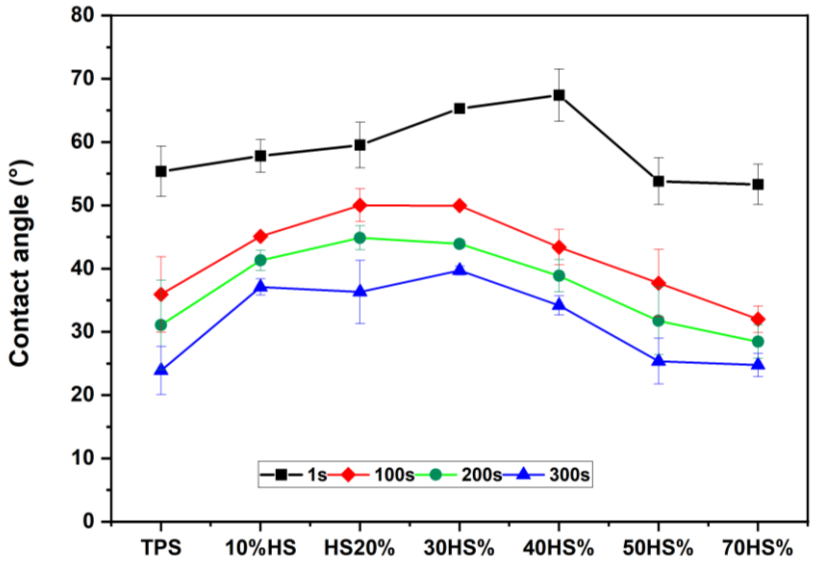

Figure 6: Contact angle for TPS and biocomposites with different HS concentrations.

Figure 7

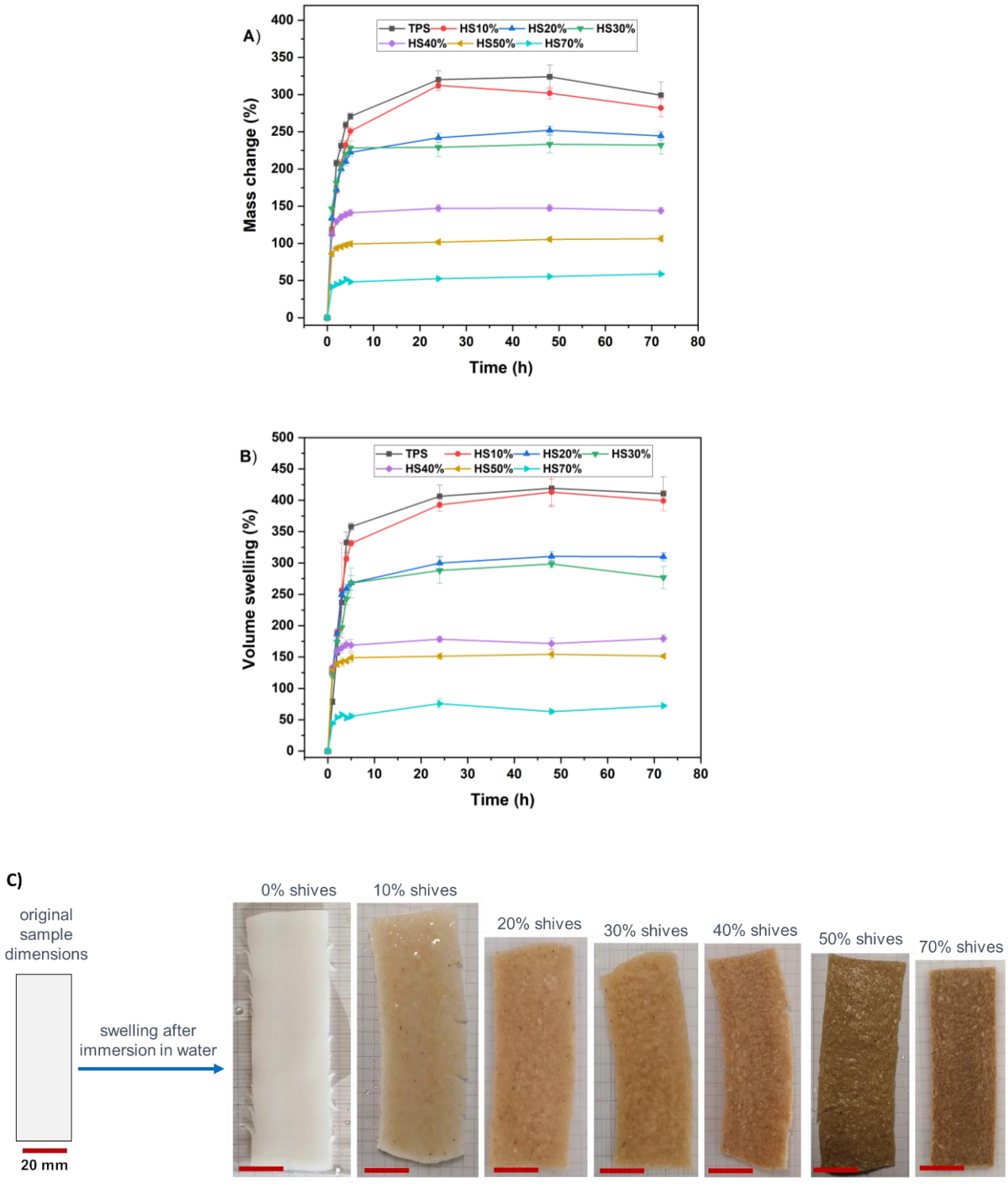

Figure 7: A) Water uptake, B) swelling volume of TPS and biocomposites with different HS contents and C) Images of TPS and biocomposites with different HS contents after an immersion time of 24 h in liquid water. The red bar indicates 20 mm. D) Moisture adsorption as function of humidity for TPS and biocomposites with different HS concentrations.

Figure 8

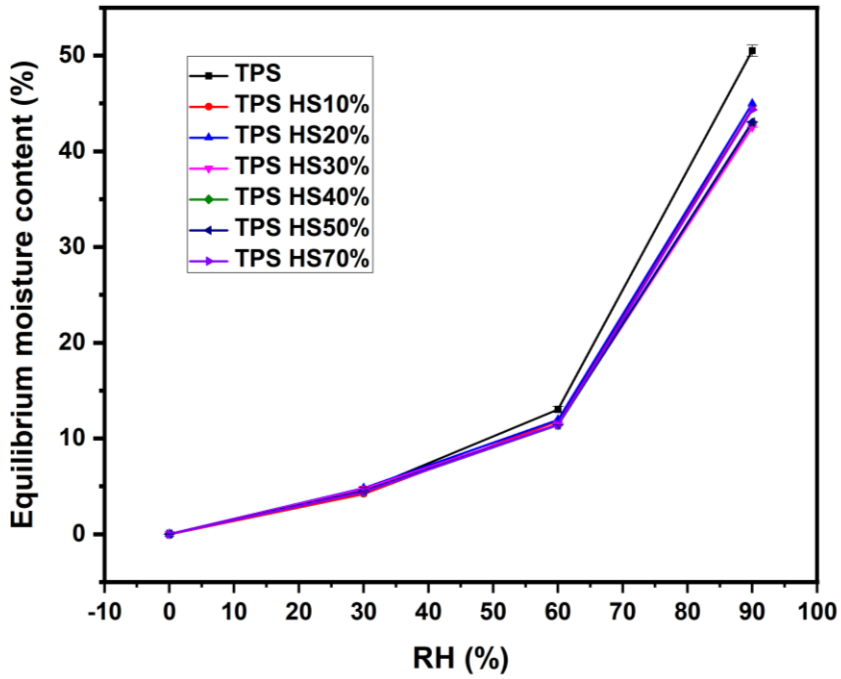

Figure 8: Moisture adsorption as function of humidity for TPS and biocomposites with different HS concentrations

Figure 9

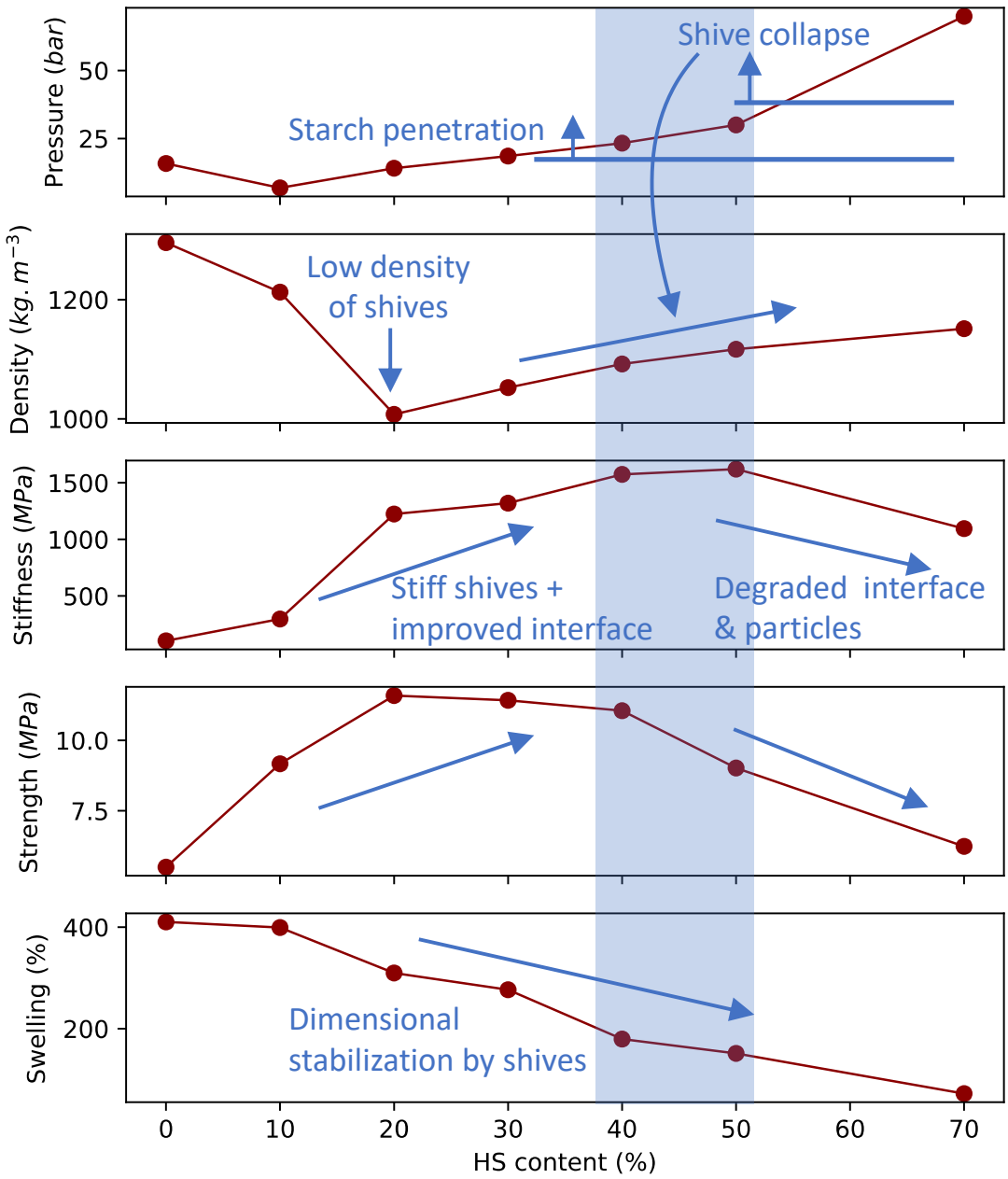

Figure 9: Summary of the effect of hemp shives content on the properties of hemp-starch composites.

Supplementary material

Table 1S: Summary of the effect of hemp shives content on the properties of hemp-starch biocomposites

	TPS	**TPS HS10%**	**TPS HS20%**	**TPS HS30%**	**TPS HS40%**	**TPS HS50%**	**TPS HS70%**
Pressure (bar)	15.8 (2.5)	6.9 (4.0)	14.1 (2.0)	18.5 (3.3)	23.3 (3.2)	30.1 (4.5)	69.9 (9.4)
Density (kg/m^3)	1095.6 (60.1)	1212.6 (16.4)	1007.6 (60.7)	1052.5 (45.8)	1092.1 (45.8)	1116.7 (36.8)	1151.4 (44.4)
Tensile strength (MPa)	5.5 (0.8)	9.2 (0.7)	11.6 (1.3)	11.4 (1.8)	11.0 (1.8)	9.0 (1.1)	6.2 (2.9)
Young's modulus (MPa)	104.4 (35.5)	296.5 (104.6)	1224.7 (105.8)	1319.9 (182.2)	1571.6 (334.9)	1621.0 (354.5)	1095.0 (341.7)
Swelling (%)	410.3 (27.3)	399.3 (16.1)	309.9 (6.5)	276.8 (17.4)	179.6 (5.8)	151.5 (1.9)	72.3 (1.6)
Water uptake (%)	299.3 (17.5)	282.0 (11.8)	244.6 (5.7)	232.2 (12.3)	143.9 (4.1)	106.3 (4.0)	58.8 (1.4)